Developmental Lung Malformations in Children

Recent Advances in Imaging Techniques, Classification System, and Imaging Findings

Paul G. Thacker, MD, Gary R. Schooler, MD,† Michael J. Caplan, MD,‡ and Edward Y. Lee, MD, MPH§*

Abstract: Congenital lung anomalies represent a diverse group of developmental malformations of the lung parenchyma, arterial supply, and venous drainage, which may present anywhere from the prenatal period through adulthood. It is imperative for radiologists to be aware of imaging techniques and imaging appearance of these anomalies across the pediatric age range. This review presents the spectrum of these lesions that are often encountered in daily clinical practice. Each anomaly is discussed in terms of underlying etiology, clinical presentation, and imaging characterization with emphasis on the most up-to-date research and treatment. Knowledge of these areas is essential for accurate, timely diagnosis, which aids in optimizing patient outcomes.

Key Words: congenital lung anomalies, prenatal imaging, computed tomography, magnetic resonance imaging

(*J Thorac Imaging* 2015;30:29–45)

LEARNING OBJECTIVES

After completing this CME activity, physicians should be better able to:

1. Distinguish the most commonly encountered congenital lung anomalies encountered in thoracic imaging
2. Analyze the most common anatomic locations of congenital lung anomalies
3. State other developmental anomalies associated with congenital lung anomalies

Congenital lung anomalies (CLA) have an annual incidence of 32 to 42/100,000 population[1–3] and represent a heterogenous group of developmental abnormalities yielding a wide variety of imaging and clinical manifestations. Many will be detected during early childhood, whereas others will remain occult into adulthood. It is thus imperative for radiologists to be cognizant of the proper imaging techniques and imaging appearances for each lesion to garner timely and accurate evaluation and diagnosis.

This article provides practical imaging techniques in the evaluation of CLA. In addition, this article includes up-to-date information of underlying etiology, clinical presentation, characteristic imaging findings, and current treatments. Future directions, which can lead to improved understanding and evaluation of CLA, are also discussed.

PRACTICAL IMAGING TECHNIQUES AND EVALUATION

Detailed descriptions of the imaging characteristics for each lesion are provided under the respective sections. However, usefulness analysis and description of the available imaging modalities are informative. Four modalities are currently used for the imaging evaluation of CLA, including chest radiography (CR), ultrasound (US), computed tomography (CT), and magnetic resonance imaging (MR).

CR

Despite CLA often being detected by prenatal US or MR, CR remains the initial imaging modality for the detection and characterization of these lesions postnatally, even if patients are asymptomatic. If obtainable, posteroanterior and lateral radiographs are the technique of choice. However, in a very young patient, a lateral radiograph may not be feasible, and a single anteroposterior radiograph must suffice.

Radiographic findings vary depending on the lesion type and size. However, general principles can provide a clue to the presence of a CLA and include: (1) focal opacity/mass; (2) focal lucency; (3) thoracic asymmetry; (4) vascular abnormalities; (5) airway anomalies; and (6) other congenital lesions involving the spinal column, heart, and gastrointestinal tract.[2,3] The presence of 1 or a combination of these findings may help in further imaging recommendations or sometimes point to a definitive diagnosis.

US

US has become an integral tool of maternofetal medicine and is the modality of choice for fetal screening. Fetal lungs appear uniformly hyperechoic compared with the liver. Focal increased areas of echogenicity or cyst may provide an early clue to the presence of an underlying CLA (Fig. 1). However, the first clue is often cardiomediastinal shift with the heart serving as an important landmark in the fetal chest, occupying a thoracic volume of 25% to 30% on the 4-chamber view.[4] Postnatally, US provides a widely available and radiation-free modality for CLA evaluation, usually following initial radiographs.

Optimal acoustic windows in the neonate and young child include the parasternal, transsternal, and intercostal

*Assistant Professor of Radiology and Radiological Science; ‡Associate Professor of Pathology and Laboratory Medicine, Medical University of South Carolina, Charleston, SC; †Pediatric Radiology Fellow, Department of Radiology; and §Chief of Division of Thoracic Imaging, Director of Magnetic Resonance Imaging, Department of Radiology, Boston Children's Hospital and Harvard Medical School, Boston, MA.

All authors and staff in a position to control the content of this CME activity and their spouses/life partners (if any) have disclosed that they have no financial relationships with, or financial interests in, any commercial organizations pertaining to this educational activity.

Correspondence to: Edward Y. Lee, MD, MPH, Chief of Division of Thoracic Imaging, Director of Magnetic Resonance Imaging, Department of Radiology, Boston Children's Hospital and Harvard Medical School, 300 Longwood Ave. Boston, MA 02115 (e-mail: edward.lee@childrens.harvard.edu).

CME Copyright © 2014 by Lippincott Williams & Wilkins

FIGURE 1. Coronal image through the thorax of a fetus demonstrates a triangular-shaped CPAM (X) within the left lower lobe that is hyperechoic to the adjacent normal lung (+) and heart/descending aorta (*).

approaches utilizing a high-resolution 10 to 15 MHz linear-array transducer.[5] At least 2 orthogonal planes are acquired, with Doppler used for aberrant vascularity evaluation. With increased patient age, US becomes limited because of decreased sonographic windows, and US may simply add to increased cost while providing little additional diagnostic information.

CT

After CRs, CT, specifically multidetector CT (MDCT), is generally recommended in CLA evaluation. MDCT advantages include fast acquisition times, high spatial resolution, and exquisite detail of multiplanar (MPR) and 3-dimensional (3D) reconstructions.[2,6] Disadvantages include its relatively high doses of radiation and respiratory motion in the subset of children unable to cooperate with breath-holding. These disadvantages have progressively decreased with newer-generation scanners and low-dose techniques.

Optimal scan coverage is of utmost importance for CLAs. Generally, coverage extends from the thoracic inlet to the diaphragm. In specific situations, for example, extralobar sequestration and type 2 pulmonary artery slings, coverage may be extended. Technical parameters will vary on the basis of the CT scanner model, patient size, and imaging protocol. However, some general parameters for tube current, kilovoltage, collimation, and table speed are worth considering. Given the wide range of pediatric patient sizes, both tube current and kilovoltage are varied on the basis of patient weight. For patients <10 kg, a current of 40 mA is used, whereas patients ≥ 50 kg receive between 100 and 120 mA. For patients <50 kg, 80 kVp is used, whereas in larger patients, a kVp of 100 to 120 may be needed. Table speeds of <1 second are routinely used. Collimation is dependent on detector number but is generally 0.5 to 0.6 mm for 64-detector row scanners.[6]

In addition to modulating mA and kVp, recent research has demonstrated that newer reconstruction algorithms, for example, adaptive statistical iterative reconstruction and model-based iterative reconstruction, can further reduce radiation exposure while yielding equivalent or superior image quality to filter back projection.[7] In recent pediatric studies by Singh et al[8] and Mieville et al,[9] 46.4% dose reduction was achieved with adaptive statistical iterative reconstruction with equivalent image quality to filtered back projection. Although neither study evaluated patients with CLA, it can likely be assumed that dose reduction using iterative reconstruction can be achieved without sacrificing diagnostic quality.

After the initial axial data set is acquired, 3D reformations of the lung, airway, and vascularity may be constructed. Axial images are highly accurate for the diagnosis, location, associated mass effect, and anomalous arterial supply of CLAs. In addition, MPR and 3D reconstructions have been recently demonstrated to provide added value for CLA associated with anomalous veins.[10] As such, these should be routinely generated in many cases.

MR

Given lack of ionizing radiation and high tissue-contrast resolution, MR provides an alternative for the evaluation of vascular and solid constituents of CLAs. However, MR is limited in its ability to depict lung parenchymal anomalies and, as such, serves only a secondary role to CT. Despite limitations, MR may be utilized in situations in which the risks of CT radiation outweigh the benefits, such as in the prenatal period.

Prenatal MR is often requested after an abnormal screening US. Small CLAs do not need further advanced imaging in the prenatal period. Very large lesions resulting in pulmonary hypoplasia and pulmonary compromise often do, as residual lung volume calculation has been shown to directly correlate with patient prognosis.[11]

T2-weighted single-shot rapid-acquisition sequences represent the workhorse of fetal MR imaging, providing exquisite anatomic and pathologic detail (Fig. 2). Given the fluid-filled fetal respiratory tree, the trachea, bronchi, and the lungs are T2 hyperintense relative to the chest wall. Alveolar fluid production increases with advancing gestational age, further increasing lung T2 hyperintensity. If an abnormality is detected, images with smaller fields of view are acquired. T1-weighted images are routinely obtained but may be suboptimal given the time required for acquisition. Spoiled gradient-echo imaging seems to be the most beneficial of the T1 sequences available.[2,3]

Postnatal MR protocols are tailored to the suspected lesion type. For both vascular and nonvascular CLAs, axial T1 or double inversion recovery, axial and coronal T2 fast relaxation fast spin echo, coronal 3D angiography, post-gadolinium axial and coronal T1-weighted images with fat saturation, and spoiled gradient-recalled echo after gadolinium are often acquired. For vascular lesions, additional sagittal 3D spoiled gradient-echo angiographic and 3-plane fast spin echo double inversion recovery sequences are added.

Recent studies have introduced the concept of unenhanced fast-imaging protocols for pediatric thoracic evaluation.[12,13] In a prospective study comparing unenhanced fast-imaging MR versus contrast-enhanced MDCT in 71 children, Gorkem et al[12] demonstrated MR to have an accuracy of 97% with 96% sensitivity and 100% specificity for thoracic abnormalities. Similarly, Yikilmaz and colleagues demonstrated MR with fast-imaging sequences at 1.5 T to be comparable to CRs for pediatric pneumonia. Neither study specifically evaluated CLA, although Gorkem and colleagues' study did have 1 case of a bronchogenic cyst.[13] These findings are promising and support the assumption that MR may be able to serve as a CT alternative for CLA evaluation.

 © 2014 Lippincott Williams & Wilkins

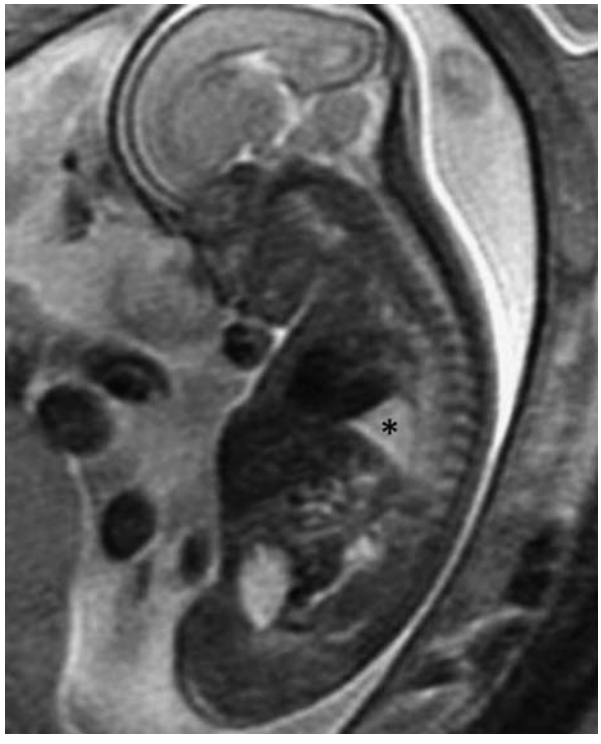

FIGURE 2. Sagittal T2 image through the fetus shows a triangular-shaped hyperintense mass (*) representing a CPAM, which resides posterior to the heart within the left lower lobe.

Postnatally, the respiratory system becomes air filled, resulting in marked trachea, bronchial, and lung hypointensity on all pulse sequences, providing little anatomic detail outside of pathologic abnormalities. However, definition of aberrant vascularity remains exquisite, particularly after gadolinium administration. It should be noted that gadolinium should only be utilized if necessary in the early neonatal period, given the relative renal insufficiency of newborn kidneys.

In addition to standard descriptive anatomic information, MR can provide useful physiological data beyond what is available by other modalities. Residual lung volumes often represent the predominant driver of morbidity and mortality in patients with large CLAs.[14] Phase contrast imaging can give useful flow dynamics within some vascular CLAs.[15]

Lastly, MR is limited in the full evaluation of the pulmonary parenchyma given the low proton density of lung tissue and resultant weak MR signal. To compensate, hyperpolarized gases, for example, ^{3}He and ^{129}Xe, have been investigated as methods to improve lung MR signal.[16–18] Thus, both structural and functional information can be obtained with ventilation imaging. However, research in children has been largely confined to those with asthma and cystic fibrosis.[18] As such, the utility of hyperpolarized gas for CLA evaluation has not yet been demonstrated.

SPECTRUM OF IMAGING FINDINGS

Branching Anomalies

Developmental Interruptive Lesions

Agenesis, Hypoplasia, and Aplasia. Fetal lung underdevelopment is classified into 3 categories: lung agenesis, lung aplasia, and lung hypoplasia.[2,3]

Currently, the cause of pulmonary agenesis and aplasia remains unknown. With pulmonary agenesis, there is complete absence of all normal pulmonary structures affecting either one or both hemithoraces. In pulmonary aplasia, a rudimentary bronchus is present, whereas the lung parenchyma and pulmonary vasculature are absent. When affecting both hemithoraces, pulmonary agenesis/aplasia is uniformly fatal. However, patients with unilateral pulmonary agenesis/aplasia may remain asymptomatic into adulthood.

In contrast, the pulmonary artery and bronchus are present but hypoplastic with a variable degree of lung parenchyma in pulmonary hypoplasia. Pulmonary hypoplasia is divided into 2 subcategories. In primary pulmonary hypoplasia, there is no identifiable cause. Secondary pulmonary hypoplasia results from limited fetal pulmonary development produced by varied intrinsic and extrinsic causes, such as congenital diaphragmatic hernia, oligohydramnios, thoracic dystrophies, and congenital pulmonary masses.[2,3]

The imaging appearance of pulmonary agenesis, aplasia, and hypoplasia is dependent on the amount of pulmonary structures present. On all imaging scans, the affected hemithorax is asymmetrically small with hemidiaphragm elevation and variable amounts of mediastinal shift. Hyperinflation of the contralateral lung may be present and can herniate across the central chest (Fig. 3).

Bronchial Atresia (BA). BA results from subsegmental or segmental bronchial obstruction with normal formation of the airway distal to the obstruction. The exact cause of the obstruction remains elusive with 2 theories proposed. One theory holds that BA results from obliteration of the connection between the primitive bronchial cells and the tip of the bronchial bud. A second theory postulates that BA results from a focal ischemic insult causing focal bronchial lumen disconnection.[3]

Historically, BA was thought to be an isolated anomaly. This is no longer the case as multiple associated congenital anomalies have recently been described. In a study by Riedlinger et al,[19] BA was present in 50% of congenital lobar emphysema (CLH) cases, 70% of congenital pulmonary airway malformations (CPAM), 82% of intralobar sequestrations, and 100% of extralobar sequestrations. The association of BA with sequestrations and CPAMs has led to the phrase "bronchial atresia sequence" to encompass this maldevelopment spectrum.[19] Generally, pediatric BA patients present with recurrent infection or respiratory distress with severity related to the degree of parenchymal disease. With little or no parenchyma involvement, patients may remain asymptomatic.

Classically described on CR, BA appears as a round or oval opacity, most commonly in the apical or apicoposterior upper lobe segments, although it may occur in any segment. These opacities represent impacted mucous distal to the atretic bronchus. With distal air trapping, a focal hyperlucency lung segment may be seen. If there is an associated congenital mass, mucus impaction and air trapping may be obscured. In this case, the CR appearance will be that of the associated mass. If additional imaging is necessary, CT is often the next modality utilized. Distal to the atretic bronchus, mucous-filled bronchi will appear as dilated, tubular opacities. Hyperinflated lung will be seen distal to the impacted bronchi and is thought to result from collateral air drift through pores of Kohn and the pulmonary interstitium[2,3,6,20,21] (Fig. 4). Current treatment involves resection because of increased infection risk.

© 2014 Lippincott Williams & Wilkins

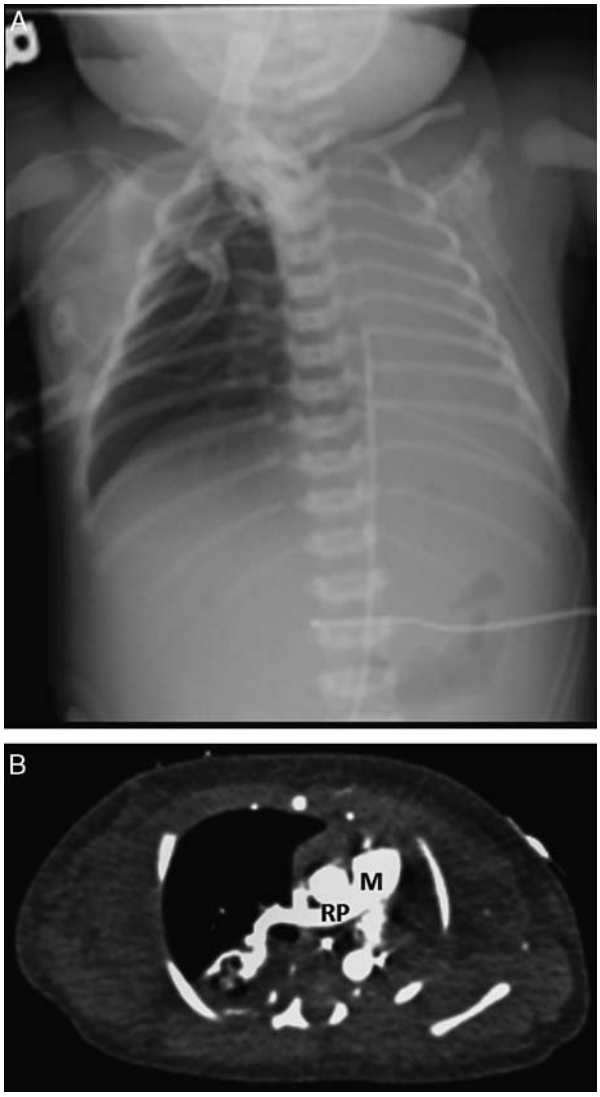

FIGURE 3. A, Frontal radiograph of the chest in a neonate shows unilateral agenesis of the left lung. The heart and mediastinal structures are shifted into the left hemithorax. Note the umbilical venous catheter, which is deviated to the left of midline, but remains within the right atrium. B, Axial image from a contrast-enhanced CT of the thorax reveals absence of the left pulmonary artery and pulmonary veins. M indicates main pulmonary artery; RP, right pulmonary artery.

Foregut Duplication Cyst. On gestational day 26, lung development begins as a ventral diverticulum from the primitive foregut. Foregut duplication cysts result from defective foregut budding and comprise a spectrum of abnormalities including esophageal duplication and bronchogenic, and neurenteric cysts. Differentiation is based on histologic examination with bronchogenic cysts containing respiratory epithelium and esophageal duplication cysts demonstrating squamous epithelium and/or pseudostratified epithelium[22] (Fig. 5A). Esophageal duplication cysts may contain other ectopic gastrointestinal tract tissue including ectopic gastric mucosa with the associated risk for hemorrhage.[23]

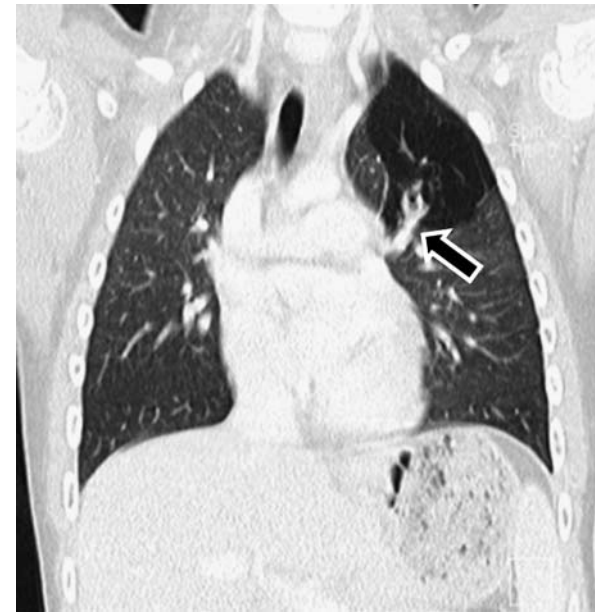

FIGURE 4. Coronal reformatted image from a contrast-enhanced CT of the thorax shows hyperlucency within the apicoposterior segment of the left upper lobe, surrounding a tubular opacity (arrow) extending to the left superior hilum, findings representing BA.

Bronchogenic cysts occur in the paratracheal, hilar, and subcarinal regions in 65% to 90% of cases, most commonly in the subcarinal region[6,24–26] (Fig. 5B). In 12% of cases, bronchogenic cysts occur intraparenchymally.[27] Esophageal duplication cysts occur in a similar distribution and may be intimately associated with the esophagus. If located in the middle mediastinum and associated with the focal cleft in the adjacent vertebral body, a neurenteric cyst may be diagnosed.

Typically, small lesions are asymptomatic and incidentally detected. With large lesions, patients may become symptomatic, often presenting with respiratory symptoms, dysphagia, or chest pain. Cysts may become infected if in continuity with the esophagus or tracheobronchial tree; this manifestation occurs more often in older children and is less common in infants and neonates.

On prenatal US, foregut duplication cysts appear as unilocular, cystic masses most commonly found in the middle mediastinum.[28] If a prenatal MR is performed, they usually manifest as well-circumscribed, smooth masses with heterogenous T1 signal and T2 hyperintensity.[4] If cystic fluid is hemorrhagic or significantly proteinaceous, duplication cysts may be uniformly T1 hyperintense.

Yet, foregut duplication cysts are often first identified on CR, manifesting as round or oval, well-circumscribed masses.[2] Splaying of the main stem bronchi may be seen. Generally, CT is performed for further evaluation once detected on CR and these lesions share a similar CT appearance as smooth, well-defined, rounded or oval masses with homogenous internal attenuation if uncomplicated (Fig. 5). Fifty percent of lesions will have CT attenuation values close to that of water.[3,6] However, variable attenuation can occur depending on cystic fluid protein content. Postcontrast, uncomplicated foregut duplication cysts have

 © 2014 Lippincott Williams & Wilkins

FIGURE 5. A, Medium-power pictomicrograph of a section from a bronchial duplication cyst view showing pseudostratified columnar epithelium and glands. B, Coronal reformatted image from a contrast-enhanced chest CT demonstrates a mediastinal mass (*) splaying the carina and resulting in obstruction of the left main stem bronchus with air trapping (arrows) in the left lower lobe. full color online

minimal or no wall or internal enhancement. With concurrent or prior infection, foregut duplication cysts may have a thick or irregular wall with more robust enhancement. Air-fluid levels may also be seen.

If infected or symptomatic, thoracoscopic or open surgical resection may be performed. Recent alternatives to surgical resection have been proposed and include percutaneous or transbronchial cyst aspiration.[2]

Ectopic or Supernumerary Bronchial Lesions

Tracheal Bronchus. First described in 1785 by Sandifort as an aberrant bronchus originating from the trachea and supplying the right upper lobe, the term tracheal bronchus now refers to multiple bronchial anomalies whereby an aberrant bronchus arises from either the main bronchi or the trachea and supplies the upper lobe territories.[29] Over the years, additional terms have been utilized. "True" tracheal bronchi originate directly from the trachea, normally within 2 cm from the carina. A displaced bronchus refers to the absence of a normal upper lobe bronchus with the tracheal bronchus supplying the entire ipsilateral upper lobe. A "pig bronchus" refers to when the right upper lobe bronchus is displaced onto the trachea. The bronchus is termed supernumerary when it supplies the ipsilateral upper lobe in additional to a normally bifurcating or trifurcating upper lobe bronchus.[30] Prevalence is 0.1% to 2% on the right and 0.3% to 1% on the left.[29,31] A displaced tracheal bronchus is more common than a supernumerary type.[32]

Affected children are usually asymptomatic. However, tracheal bronchi can be associated with recurrent upper lobe infection, bronchiectasis, or persistent upper lobe atelectasis. Tracheal bronchi may occur with other congenital anomalies including cardiac anomalies, tracheal stenosis, and in Down syndrome.[30]

Although not often apparent on CR, tracheal bronchi may appear as a tubular lucency arising from either the trachea or main stem bronchi and tracking into the ipsilateral upper lobe. An ipsilateral upper lobe opacity can be seen with superimposed infection or atelectasis. Nevertheless, tracheal bronchi are almost always first diagnosed on cross-sectional imaging. On CT, tracheal bronchi appear as a well-defined bronchus arising from the trachea or main stem bronchi and extending into the ipsilateral upper lobe (Fig. 6). Supernumerary or displaced subtyping is readily apparent by evaluating for a normal branching pattern of the main bronchi. 3D reconstructions exquisitely demonstrate the aberrant bronchial anatomy, but their definitive usefulness for treatment planning has yet to be demonstrated. MR imaging occasionally may demonstrate the presence of a tracheal bronchus as a hypointense tubular branch.

As these anomalies are usually asymptomatic, no particular treatment is normally needed. However, its presence is important to communicate in patients undergoing intubation because of the risk of occluding the bronchus. With recurrent infection, surgical resection of both the bronchus and the lobe it supplies may be necessary.[33]

Accessory Cardiac Bronchus. An accessory cardiac bronchus is a supernumerary bronchus originating from the main bronchi or bronchus intermedius and coursing in an inferior direction toward the pericardium. Most end blindly. Overall frequency in the population is approximately 0.08%.[29] Accessory cardiac bronchi are often asymptomatic. In older children, they may serve as a source of recurrent infection, and affected patients can present with cough and hemoptysis.[29] Cases of aspergillomas and tumors within accessory cardiac bronchi have been reported.[29,34,35]

The role of CR is limited. If infection or tumor is present, a focal soft tissue opacity may be demonstrated, most commonly in the subcarinal region. Still, cardiac bronchi are almost always first demonstrated on CT. Here, cardiac bronchi will appear as a focal accessory bronchus arising from the inferior aspect of the main stem bronchi or the medial wall of the bronchus intermedius. These anomalies then course inferiorly to the adjacent pericardium where they abruptly end in a blind pouch. Infection or tumor appears as a focal opacity at the tip or surrounding the cardiac bronchus.

No treatment is necessary for uncomplicated accessory cardiac bronchi. If recurrent infection develops or tumor is present, a thoracotomy with surgical resection is warranted.

© 2014 Lippincott Williams & Wilkins

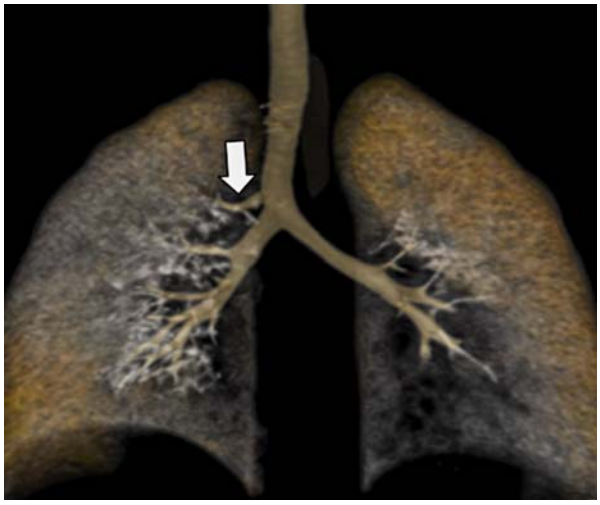

FIGURE 6. Anterior view from a volume-rendered 3D CT image of the lungs and airway demonstrates the entire course of a tracheal bronchus (arrow) and its relationship to the distal trachea. full color online

Parenchymal Anomalies

Congenital Lobar Hyperinflation (CLH)

CLH, also known as congenital lobar emphysema and congenital lobar overinflation, results from intrinsic or extrinsic narrowing of the bronchial lumen and manifests as overinflation of 1 or multiple pulmonary lobes.[2,3] Absence or weakness of bronchial cartilage represents intrinsic causes of bronchial narrowing.[2] Extrinsic etiologies include enlarged or aberrant vessels and mediastinal masses.

There are 2 classifications of CLH predicated on alveolar number. Hypoalveolar CLH has fewer than expected alveoli with alveolar overdistension. In polyalveolar CLH, the number of alveoli is increased 3- to 5-fold in the affected lung segment with each individual alveolus normally inflated (Fig. 7A). Thus, the affected lobe(s) are overinflated because of the increased number of normally inflated alveoli.[2,3] Presentation often depends on type, with hypoalveolar CLH presenting earlier in life. Respiratory distress is what typically brings patients to clinical attention, with severity dependent on the amount of hyperinflation and associated compression of mediastinal structures and adjacent lung.[2,6] CLH is often detected during the neonatal period and has a distinct lobe predilection. The most common site is the left upper lobe, with the right middle lobe being the next most common followed by the right upper lobe (Fig. 7B). Lower lobe involvement is uncommon. Rarely, CLH may be bilateral or multifocal.[36]

On fetal US, CLH manifests as a hyperechoic, homogenous mass with variable associated compression of the adjacent normal lung and mediastinal structures. On fetal MR imaging, CLH presents as a homogenous, T2-hyperintense mass.[4] With CR, CLH demonstrates a classic temporal progression in the early neonatal period. Early on, CR will show a focal mass-like opacity resulting from retained fetal fluid. As fetal fluid is cleared, there is progressive hyperlucency of the affected lobe(s). The affected lobe(s) may become increasingly overdistended with increasing compression of the adjacent lung and mediastinum. If detected past the neonatal period, CLH may be confused with CPAM. Here, CT can be useful for further characterization and differentiation. In large CLH lesions, the affected lobe(s) will be hyperinflated with displacement of the pulmonary vessels, compression of the adjacent lung, and contralateral mediastinal shift. Ipsilateral hemidiaphragm compression and rib interspace splaying may be seen.[6]

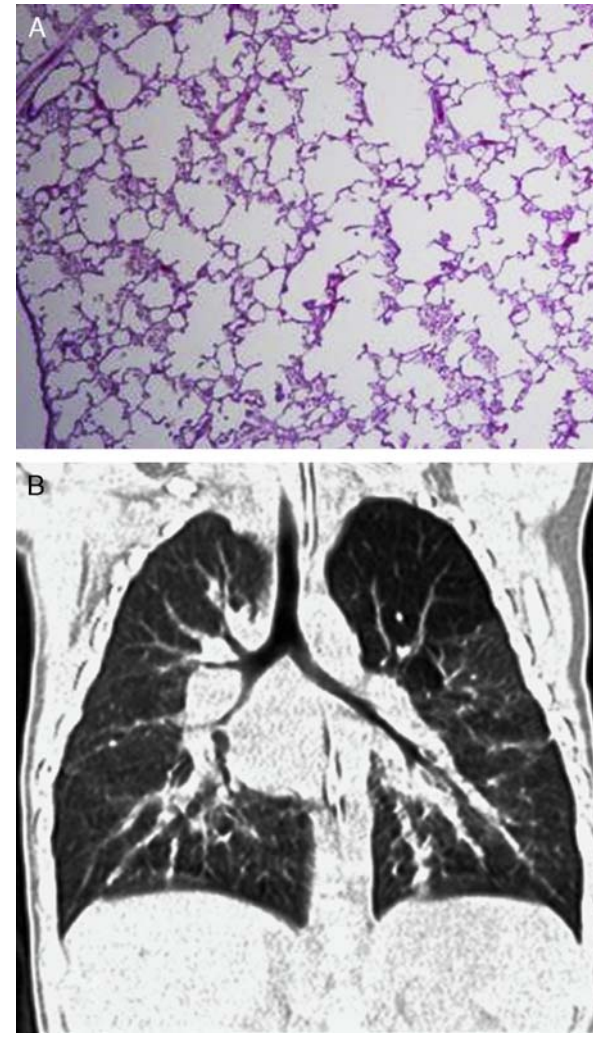

FIGURE 7. A, Pictomicrograph at low-power magnification reveals an increased number of alveoli, which are normally inflated and without features of maldevelopment consistent with polyalveolar CLH. B, Coronal reformatted CT image demonstrates hyperlucency of the left upper lobe in this patient with CLH. full color online

CLH is treated surgically, with timing dependent on lesion size and the degree of respiratory compromise.[6,37–40] Care must be taken during operative ventilation to avoid preferential aeration of the affected lobe with associated progressive hyperinflation and respiratory/cardiovascular collapse from tension physiology. With successful surgical resection, patients have an excellent prognosis.[39]

CPAM

CPAMs are a heterogenous group of cystic and noncystic anomalies and are the most common CLA,

 © 2014 Lippincott Williams & Wilkins

representing about 30% to 40% of cases.[41–44] CPAMs are thought to result from early airway maldevelopment from intrauterine airway obstruction,[2,4] supported by histologic and pathologic changes of exuberant primary bronchiolar overgrowth in communication with an abnormal bronchial tree lacking cartilage.[2,24,32,37,45–47] Arterial supply normally arises from the pulmonary artery with pulmonary venous drainage. Patients present early in life with respiratory distress. If presenting in later life, they often manifest as recurrent infection involving the same segment of the lung. However, a substantial portion of CPAMs may remain asymptomatic throughout life and are only incidentally detected.

CPAM classification was first proposed by Stocker et al in 1977[46] and was recently updated by Stocker,[47] expanding from 3 to 5 types. With this expansion, the old nomenclature of cystic adenomatoid malformations was replaced by CPAM. This term is more accurate given that only 3 of 5 types are cystic and only 1 type has adenomatoid changes. The revised Stocker classification includes 5 types (0 to 4), with classification predicated on histologic similarities to the developing bronchial tree and airspace as well as cyst size.[47] Type 0 CPAMs have severe acinar dysgenesis affecting all lung lobes and are uniformly fatal. Solitary or multiple macrocysts (>2 cm) characterize type 1 CPAMs and are of bronchial or bronchiolar origin (Fig. 8). Type 2 CPAMs have single or multiple cysts of bronchiolar origin measuring between 0.5 and 2 cm (Fig. 9). Type 3 CPAMs have multiple microcysts measuring $\leq$0.5 cm and are predominately solid. This type is the only adenomatoid CPAM type and has a bronchiolar-alveolar duct origin. Type 4 CPAMs have a distal acinar origin and are characterized by large air-filled cysts. Type 4 CPAMs are indistinguishable by imaging from type 1 pleuropulmonary blastoma.[2,4,47]

CPAMs are often first identified on prenatal US. On US, the overall mass size and associated compressive effects on the adjacent normal lung and mediastinal structures may be assessed. In some cases, CPAMs may be subcategorized prenatally, adding important prognostic value. Types 1 and 2 (macrocystic) CPAMs appear on prenatal US as echogenic masses with variable-sized cysts.[4] Type 3 CPAMs are indistinguishable on prenatal US from other solid CLAs, appearing as a homogenous echogenic mass. Occasionally, associated anomalous vascularity may be

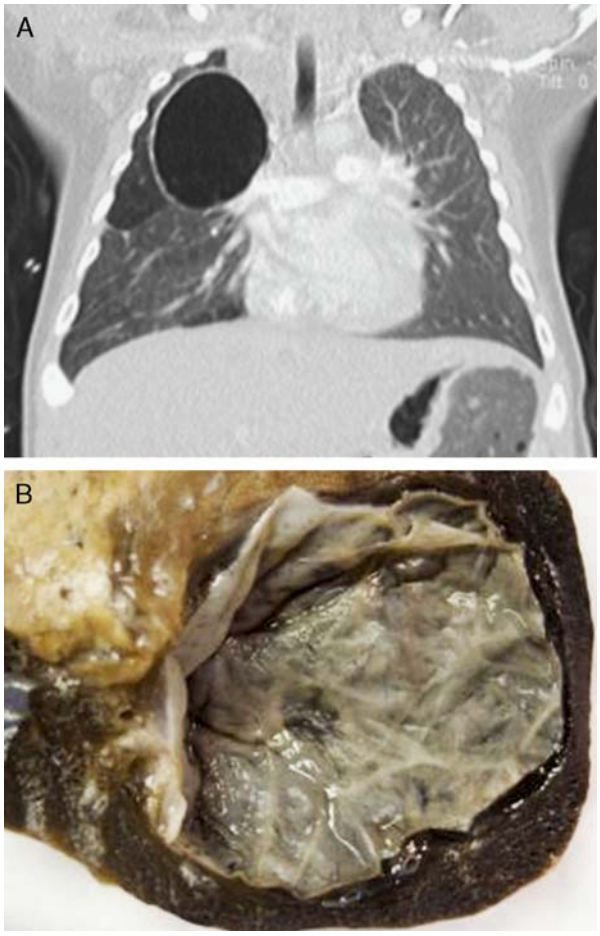

FIGURE 8. A, Coronal reformatted image from a contrast-enhanced CT of the thorax in a patient with a type 1 CPAM shows a large air-filled cyst within the right upper lobe. B, Gross surgical specimen showing a large cyst with a trabeculated wall in a type 1 CPAM.

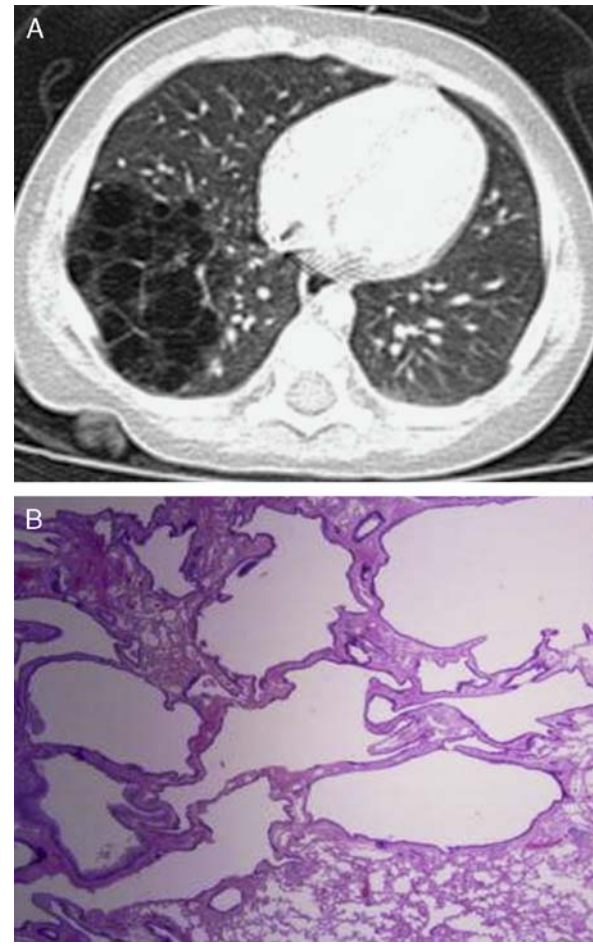

FIGURE 9. A, Axial image from a contrast-enhanced CT of the thorax in a different patient with a type 2 CPAM reveals a multicystic mass in the right lower lobe. Note that none of the air-filled cysts measure >2 cm in diameter. B, Low-power magnification view of microcystic, dilated bronchiole-like structures in a type 2 CPAM.

© 2014 Lippincott Williams & Wilkins

seen. In such cases, a hybrid lesion is diagnosed (further discussed below).

CRs are often utilized in the postnatal period, and imaging manifestations are dependent on the underlying type. The single exception to this principle is type 0 CPAMs, which generally receive no postnatal imaging given the rapidly deteriorating clinical course. On CR, type 1 CPAMs appear as a mixed solid and cystic lung mass with at least 1 cyst measuring >2 cm. If a single large/dominant cyst is present, they may be difficult to distinguish from CLH. Similarly, type 2 CPAMs are mixed cystic lung masses with cysts measuring 0.5 and 2 cm.[4,47] Alternatively, type 2 CPAMS may manifest as a persistent area of consolidation with cysts only demonstrable on cross-sectional imaging.[2] Much like their prenatal sonographic appearance, type 3 CPAMs appear on CR as solid-appearing focal opacities indistinguishable from other solid CLAs. Type 4 CPAMs are indistinguishable from type 1 pleuropulmonary blastomas, appearing as a large cystic lesion.

After initial chest radiographs, CT or MR imaging is often utilized for further characterization and treatment planning. With these modalities, the imaging appearance closely correlates with that of their CR appearance with cyst presence and size determining type classification (Fig. 8A). These cysts may be completely air filled or contain air-fluid levels.[6] On MR, if the cysts are fluid filled, typically the fluid is hyperintense on T2. Conversely, if the cysts are air filled, they usually appear diffusely hypointense on all pulse sequences. Type 3 CPAMs are composed of innumerable microcysts, which are in general not individually discernible on CT or MR. Thus, type 3 CPAMs almost always appear on CT and MR as a focal solid lesion with diffuse homogenously increased T2 signal on MR.[4]

Treatment for symptomatic patients is operative, which is now often performed via thoracoscopy with either a lobectomy or segmentectomy performed. Treatment for asymptomatic patients remains controversial. Most believe that elective resection is prudent given the associated risks of hemorrhage, recurrent infection, and potential risk for malignancy.[6]

Vascular Anomalies

Anomalies of the Pulmonary Artery

Interruption (Absence) of a Main Pulmonary Artery. The primitive sixth aortic arch gives rise to the proximal aspect of the main pulmonary artery. Failure of the formation of the sixth aortic arch results in proximal interruption of the pulmonary artery. Given their differing embryological origin, the hilar and distal pulmonary arteries form normally.[6,48–51] Vascular supply to the affected lung results from collateralization of flow through bronchial and intercostal arteries with enlargement of the contralateral pulmonary vessels. However, overall flow to the affected lung is diminished, resulting in ipsilateral pulmonary hypoplasia. Venous drainage of the affected side is usually normal.[6] Patients typically present with hemoptysis from bronchial arterial enlargement, pulmonary hypertension, or recurrent infection, although patients may remain asymptomatic.[50,51]

Proximal interruption of the pulmonary artery may manifest in a similar manner on CR as mild to moderate pulmonary hypoplasia with small lung size, volume loss, and mediastinal shift. The intraparenchymal vascularity is diminished, and the ipsilateral hilum may appear small or absent. With collateralized arterial supply, there may also be increased peripheral reticular vascular markings. On CT, the focal absence of the proximal pulmonary artery is shown to best advantage with termination of the pulmonary artery usually within 1 cm of its origin from the main pulmonary artery. Recently, MDCT angiography with 3D reconstructions has been shown to have particular utility in depicting not only the focal discontinuity of the pulmonary artery but also the extent of arterial collateralization, contralateral pulmonary artery enlargement, and associated central airway anomalies.[10]

Early treatment is key, as it may improve affected lung and pulmonary arterial growth. Surgical intervention consists of grafting or direct anastomosis of the main and hilar pulmonary artery segments. In older patients presenting with recurrent hemoptysis or pulmonary hypertension, embolization of collateral vessels may be warranted.[2,6]

Anomalous Origin of the Left Pulmonary Artery From the Right. If the left sixth aortic arch is completely obliterated during development, the left pulmonary artery may arise anomalously from the posterior right pulmonary artery. This rare congenital anomaly is commonly referred to as a pulmonary sling, with the term sling deriving from the left pulmonary artery having a looping appearance around the trachea as it passes between the trachea and esophagus from right to left. Patients generally present at an early age with upper and lower respiratory symptoms including episodic apnea, stridor, and respiratory distress.[2,3]

Anomalous origin of the left pulmonary artery from the right occurs in 2 varieties. Type 1 is associated with a normally positioned carina at the T4 to T5 vertebral level, with characteristic compression of the posterior tracheal wall, anterior esophageal wall, and the right main stem bronchus. In type 2 pulmonary artery slings, the trachea is elongated with inferior carinal displacement, generally to the T6 level. The carina takes on a T-shaped morphology whereby the main bronchi arise perpendicularly from the carina giving them a horizontal course. In 50% of cases, there is diffuse tracheal stenosis with complete cartilaginous rings. Fifty percent of patients with a type 2 pulmonary sling will have congenital heart defects.[52]

Pulmonary sling imaging manifestations are dependent on type and associated anomalies. Classically, on contrast esophagram there is an external impression on the posterior aspect of the trachea and the anterior aspect of the esophagus, the only vascular anomaly to cause this appearance. A complete vascular ring is formed when a ligamentum arteriosum is present, encircling and compressing the trachea while sparing the esophagus.

On CR, the right lung may be hyperinflated owing to right main stem bronchus compression. On the lateral radiograph, the posterior tracheal wall may be compressed by a soft tissue opacity interposed between the trachea and bronchus, with anterior tracheal displacement. MDCT with 3D reconstructions have been shown of value in the evaluation of pulmonary slings and is the current imaging modality of choice[6,10] (Fig. 10). MDCT demonstrates the anomalous origin and course of the left pulmonary artery. 3D reconstructions of the airway demonstrate the configuration and extent of tracheal stenosis. Paired inspiratory and expiratory views are of great value in demonstrating associated tracheomalacia. In type 1, both axial and sagittal images can demonstrate the anterior esophageal impression and compression of the posterior tracheal wall. With

 © 2014 Lippincott Williams & Wilkins

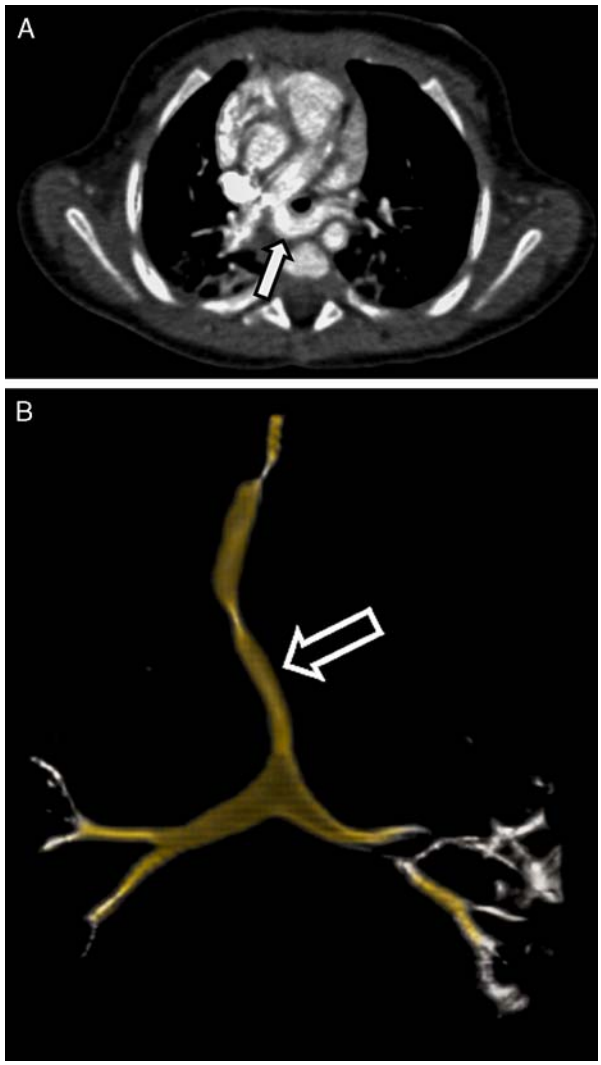

FIGURE 10. A, Axial image from a contrast-enhanced CT of the thorax reveals the aberrant left pulmonary artery (arrow) arising from the right pulmonary artery in a patient with a pulmonary artery sling. The pulmonary artery courses posterior to the trachea and anterior to the esophagus to reach the left lung. B, Anterior view from a volume-rendered 3D image of the trachea and proximal bronchi shows diffuse narrowing of the intrathoracic trachea (arrow) due to complete cartilaginous rings and a "T-shaped" configuration of the carina characteristic of a type 2 pulmonary artery sling. full color online

intravenous contrast, the looping anomalous course of the left pulmonary artery can be seen. Associated right lung hyperinflation is best depicted with expiratory images.[6] CT features of a type 2 pulmonary sling include a T-shaped carina with caudal displacement of the carina to the T6 level. Long-segment tracheal stenosis may be demonstrated and is seen to best advantage on coronal reformations and 3D reconstructions (Fig. 10B). When assessing type 2 pulmonary slings, it is prudent to image the entire course of the trachea, as the stenosis can be diffuse. Demonstrating the extent of stenosis is helpful for planning surgical intervention.[6]

Although less often utilized, MR imaging can readily demonstrate the left pulmonary artery's anomalous origin and course. Right lung hyperinflation can be detected by asymmetric hemithorax volumes. Tracheal narrowing can also be depicted, although generally with less definition than that seen on MDCT.

Surgical division and reimplantation of the left pulmonary artery is the treatment of choice. With long-segment tracheal stenosis, tracheoplasty may be necessary. Alternatively, stenosis resection with end-to-end anastomosis may be utilized for short-segment tracheal stenosis.[53,54]

Anomalies of the Pulmonary Vein

Pulmonary Vein Stenosis (PVS). Etiologies for PVS include both acquired and congenital causes. Congenital lesions can be life threatening and are rarer, resulting from uncontrolled fibroblast growth with thickening and narrowing of the pulmonary vein.[6] Pediatric patients often present with symptoms of pulmonary edema such as shortness of breath, cyanosis, and fatigue.

Correlating with patient symptomatology, CR demonstrates signs of reduced pulmonary venous drainage, pulmonary venous hypertension, and pulmonary edema. Recently, Mayhew et al[55] evaluated CR findings in 41 infants with known PVS. The most common CR findings included increased interstitial opacity (100%), reticular opacity (85%), and ground-glass opacity (71%). Although these are nonspecific signs of pulmonary edema, given the population age and the very high percentage of these findings, the authors concluded that PVS should be considered particularly when these findings are heterogenous or unilateral.[55]

Although PVS may be depicted on MR, CT is often utilized for cross-sectional imaging as it better demonstrates associated lung parenchymal changes. The affected pulmonary venous segment is usually at or near its junction with the left atrium (Fig. 11). With disease progression, pulmonary vein thickening and narrowing may extend into adjacent distal intraparenchymal pulmonary vein segments. Pulmonary parenchymal changes follow that of unilateral pulmonary edema. Recently, the utilization of 3D reconstructions in the pediatric population has been shown to significantly increase diagnostic accuracy, diagnostic value, confidence level, and intraobserver agreement.[56]

Due to the potential life-threatening consequences of PVS, accurate and prompt diagnosis is paramount. Treatment strategies depend on disease extent. Focal or short-segment PVS is treated with percutaneous balloon dilatation and stenting. In long-segment stenosis, lung transplantation may be required.

Partial Anomalous Pulmonary Venous Return (PAPVR). PAPVR occurs when 1 or more pulmonary veins retain an embryologic connection to the primitive splanchnic system of cardinal veins.[57] The anomalous drainage pattern is varied, and these anomalous veins may drain into the vena cavae, the coronary sinus, azygous vein, a persistent left vertical vein, or directly into the right atrium. A concurrent sinus venosus defect may be present, particularly in patients with right upper lobe PAPVR.[52] PAPVR results in a right to left shunt. If hemodynamically significant, patients will present with symptoms of pulmonary overcirculation and pulmonary hypertension.

Imaging findings of PAPVR are dependent on location and number of the anomalous pulmonary vein/veins, where the veins drain, and findings of pulmonary overcirculation. In general, CRs are limited for the evaluation of PAPVR (with the exception of scimitar syndrome—discussed later). In the presence of a hemodynamically significant shunt,

© 2014 Lippincott Williams & Wilkins

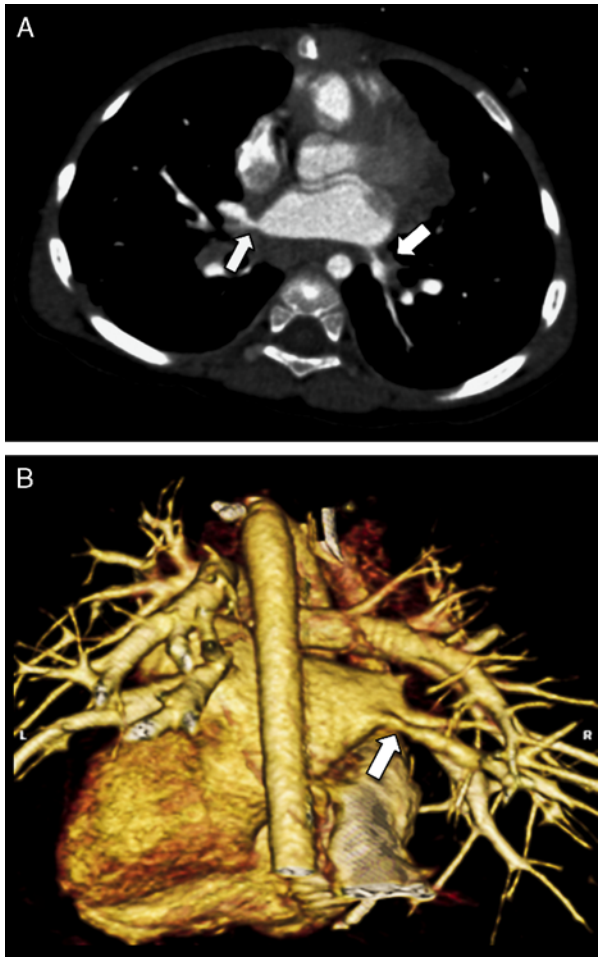

FIGURE 11. A, Axial image from a contrast-enhanced CT of the thorax in a patient with PVS demonstrates narrowing (arrows) near and at the level of pulmonary vein insertion involving veins from both lungs. B, Posterior view from volume-rendered 3D CT image from the same patient shows narrowing (arrow) of the left pulmonary vein. full color online

CRs may demonstrate pulmonary arterial and right heart enlargement.

Both CT and MR can clearly demonstrate the number and course of the anomalous pulmonary veins (Fig. 12). The most common PAPVR involves a vertically oriented anomalous left upper lobe pulmonary vein, which courses lateral to the aortic arch with drainage into the left innominate vein. This type is also the most common to not have an associated congenital heart lesion.[52,58] CT and MR can also demonstrate the associated sinus venosus defect, appearing as a focal defect in the posterior-superior atrial septum. On CT, intermixing of contrast-enhanced and noncontrasted blood across this defect may be demonstrated. On MR, a jet flow void may be demonstrated to pass through the defect.

PAPVR is usually associated with an excellent prognosis. Surgical correction with patch placement is performed if a sinus venosus defect is present. If the anomalous drainage is to the superior vena cava, the patch can be extended to separate the pulmonary from systemic drainage.[30]

FIGURE 12. Coronal image from contrast-enhanced MR angiography demonstrates drainage of the upper and middle lobe pulmonary veins (arrow) into the superior vena cava just above the level of the right atrium, findings consistent with partial anomalous pulmonary venous return.

Combined Anomaly of the Pulmonary Artery and Pulmonary Vein

Pulmonary Arteriovenous Malformation (AVM). AVMs are a consequence of a segmental maldevelopment of pulmonary capillaries resulting in direct communication of a pulmonary arterial branch with its associated/adjacent pulmonary vein. An alternative and more accurate term for pulmonary AVMs is pulmonary arteriovenous fistulae. Nevertheless, common convention refers to these lesions as pulmonary AVMs.

Pulmonary AVMs are most often congenital with a small population being acquired, typically in patients with chronic liver disease, those who have had prior surgery for congenital heart disease, and in patients with prior atypical infection, for example, tuberculosis.[3,6,59–63] Congenital AVMs are classically associated with Osler-Weber-Rendu, also known as hereditary hemorrhagic telangiectasis (HHT), an autosomal dominant disorder.

Patients with HHT often come to clinical attention due to symptoms or for screening in the setting of an HHT family history. The classic symptom triad includes epistaxis, family history, and telangiectasias, particularly nasal. Stroke or cerebral abscess may occur from right to left shunting. Thirty-five percent of HHT patients have 1 or more pulmonary AVMs[3] and may also have AVMs in other organs such as the liver, pancreas, and gastrointestinal tract.

Pulmonary AVMs manifest on CR as nodular or lobulated well-circumscribed soft tissue opacities, with 50% to 70% occurring in the lower lobes.[6] Solitary or multiple AVMs may be present. Occasionally, a tubular or curvilinear opacity may be seen to extend from the lesion with a course directed toward the ipsilateral hilum, representing the draining vein, the feeding artery, or both. Generally, the intraparenchymal nature of these lesions is apparent,

 © 2014 Lippincott Williams & Wilkins

although pulmonary AVMs may project over the mediastinum on both frontal and lateral projections, making exact localization difficult.[3]

After CR, MDCT is often performed and represents the modality of choice for assessing number, size, and location as well as the associated vascular supply. Contrast-enhanced examinations are preferable. However, AVMs may be seen on noncontrast CT obtained for alternative reasons and manifest as a focal, serpiginous or lobulated, intraparenchymal soft tissue nodule or mass. On post-contrast imaging, pulmonary AVMs robustly enhance, and the feeding and draining vascular pattern becomes readily apparent. In lesions with complex angioarchitecture, 2D-MPR and 3D reconstructions may be valuable in fully elucidating the vascular supply (Fig. 13).

The quantity of right to left shunting through pulmonary AVMs is the predominant driver of both symptoms and need for intervention. Generally, treatment is offered when feeding arteries reach a diameter of 3 mm or greater, even if asymptomatic. Treatment options include balloon occlusion, coil embolization, and surgical excision.

Combined Lung and Vascular Anomalies

Hypogenetic Lung (Scimitar) Syndrome

Hypogenetic lung syndrome, classically known as scimitar syndrome, consists of right-sided PAPVR, right lung hypoplasia, heart dextroposition, and anomalous right lung systemic arterial supply.[4,6,24,32,64] The anomalous pulmonary vein may drain into the portal venous system, the hepatic venous system, or, most commonly, the inferior vena cava. Other congenital anomalies are common and occur in up to 25% of cases.[2] Clinical presentation is dependent on patient age. Older children often present with recurrent infection in the right base. Young infants often present with symptoms of right to left shunting and pulmonary overcirculation from the anomalous pulmonary venous drainage. Some patients may remain asymptomatic.

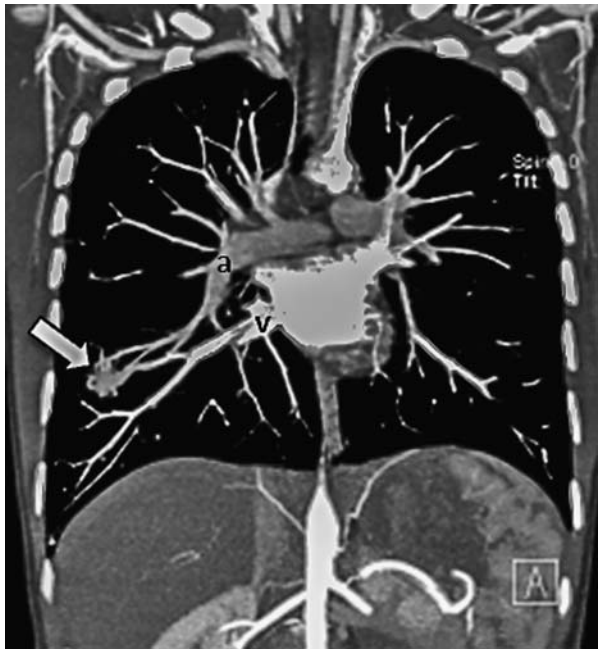

FIGURE 13. Coronal reformatted maximum intensity projection CT image in an HHT patient reveals a right lower lobe pulmonary AVM (arrow) with its associated feeding pulmonary artery (a) and draining pulmonary vein (v).

Scimitar syndrome is largely detected postnatally, although there are a few reports within the literature describing prenatal detection.[65–67] CR often is the first postnatal imaging study. Unlike many of the aforementioned anomalies, scimitar syndrome is rather unique in that its definitive diagnosis can be made by the radiograph alone. The anomalous pulmonary vein appears as a curvilinear, tubular soft tissue opacity coursing in a vertical orientation in the lower right hemithorax. The right hemithorax is small in size, and the right lung is hypoplastic and hyperlucent (Fig. 14).

Despite the ability of CRs to make the definitive diagnosis, most patients undergo cross-sectional imaging, that is, CT or MR. CT and MR are beneficial in demonstrating the anomalous pulmonary vein course, caliber, and drainage pattern. The scimitar vein most commonly drains into the inferior vena cava and less commonly into the hepatic veins, portal veins, right atrium, superior vena cava, and the azygous vein.[3,6,32,42,68] With angiographic technique, the anomalous arterial supply may also be demonstrated. 3D reformations are helpful in demonstrating both the venous and arterial anomalies in a single image.[6] Other associated nonvascular anomalies are readily demonstrated on CT including hypoplasia of the right lung with altered lobulation and bronchial branching anomalies.[2,6,69] Postoperatively, CT is helpful in evaluating reimplantation complications, for example, thrombosis and stenosis.

Treatment is largely reserved for symptomatic patients, especially with a left to right shunt ratio $>2:1$. The anomalous systemic arterial supply is often embolized with surgical reimplantation of the anomalous pulmonary vein to the left atrium.[2,6]

Pulmonary Sequestration

Pulmonary sequestrations represent the second most common congenital pulmonary anomaly.[4] It is composed of dysplastic pulmonary tissue, contains no normal connection to the tracheobronchial tree, and receives a systemic vascular supply.[2–4,6,32,42,48,70–72] Pulmonary sequestrations are traditionally divided into 2 categories, that is, intralobar versus extralobar, on the basis of its venous drainage pattern and pleural investment. Intralobar sequestrations comprise 75% of sequestrations. They do not have their own pleural investment but rather share pleura with the adjacent normal lung. Generally, intralobar sequestrations drain through the ipsilateral pulmonary venous system.[4] It remains controversial whether or not these represent true congenital anomalies in all cases, with some authors arguing that they are acquired as a result of recurrent localized infection, resultant bronchial obstruction, and eventual parasitization of the adjacent systemic vascular supply. However, with prenatal imaging advances, evidence supports that at least a subcategory is congenital as there has been increased detection of intralobar sequestrations in the fetal lungs. In contrast, extralobar sequestrations are generally considered to be a congenital anomaly and account for 25% of sequestrations.[2,3,6,32,48,70,72] Extralobar sequestrations drain through the systemic venous system and contain their own pleural investment. Regardless of type, pulmonary sequestrations receive a systemic arterial supply

© 2014 Lippincott Williams & Wilkins

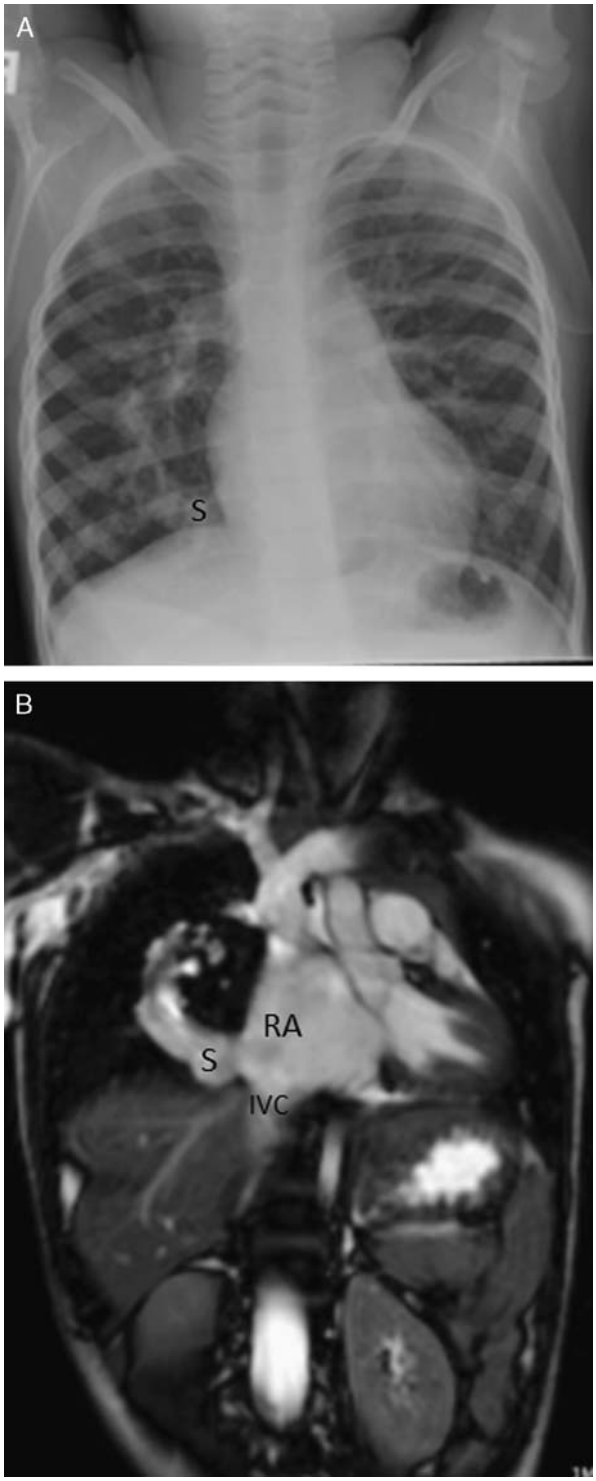

FIGURE 14. A, Frontal chest radiograph demonstrating a large anomalous pulmonary vein (S). B, Coronal T2-weighted image shows the anomalous pulmonary vein (S) draining into the junction of the inferior vena cava (IVC) and right atrium (RA).

most commonly directly from the thoracic or abdominal aorta with less common supply from the celiac, splenic, intercostal, subclavian, and coronary arteries.[4,48]

The presentation depends on the sequestration type. Extralobar sequestrations most often present in the neonatal period or in early infancy as a focal mass on imaging. Intralobar sequestrations present later in childhood as a focus of recurrent infection.[2,6,32,48,70,72]

Like most congenital pulmonary anomalies, but particularly with pulmonary sequestrations, imaging plays a key role in diagnosis and surgical planning. On prenatal US, sequestrations appear as a hyperechoic homogenous lesion, most commonly in the lower left hemithorax.[4] Doppler may demonstrate systemic arterial supply distinguishing sequestrations from other CLAs. Sequestrations appear on prenatal MR as a homogenous T2-hyperintense mass. Although gadolinium is often not utilized, the arterial supply may be seen as a serpiginous, tubular signal void arising from the aorta.[4,42]

After the prenatal period, the imaging appearance of sequestrations is more variable and depends on type, concurrent or prior infection, and other anomalies. US has a limited role postnatally. However, it does have value and may be utilized to demonstrate the aberrant arterial supply to a prenatally detected mass and confirming the diagnosis. Depending on institutional and surgeon preferences, additional imaging may not be obtained. However, a large majority of patients have a postnatal CR, often followed by CT.

Pulmonary sequestrations appear as a focal opacity or mass in the lower lobe in 98% of CRs.[6,32] Occasionally, the aberrant systemic artery may be demonstrable.[24] With recurrent infection, intralesional necrosis may develop, and a more cystic appearance with or without air-fluid levels may be seen.[2,6]

After the initial CR, MDCT with 3D reconstructions is generally utilized for both diagnosis confirmation and presurgical planning (Fig. 15). The mass itself can have a variable appearance ranging from a complex cavitary mass with intracystic air-fluid levels to a heterogenously enhancing solid lesion. In 50% of cases, sequestrations can be categorized into intralobar and extralobar on the basis of the venous drainage pattern.[73,74] Extralobar sequestrations most commonly drain into the azygous system and less commonly through the portal system, subclavian veins, and internal mammary veins.[6,70,73] Intralobar sequestrations typically drain through the inferior pulmonary vein.[6] A recent study consisting of 46 pediatric patients showed that axial CT images allow accurate diagnosis of the types, location, associated mass effect, and anomalous arteries of CLAs. However, supplemental MPR and 3D MDCT images add additional diagnostic value.[10]

A variant of sequestration known as a hybrid lesion is worth noting. Hybrid lesions represent a midpoint on a spectrum between CPAMs and pulmonary sequestrations. On CT, hybrid lesions show characteristics of a CPAM while having an anomalous systemic arterial supply.

MR and MR angiography provide nonradiation alternatives for the evaluation of pulmonary sequestrations. However, they are less often utilized given the limited definition of pulmonary parenchyma. Depending on the history of infection, sequestrations appear on postnatal MR as solid lesions with both T1 and T2 hyperintensity, which is considered to result from internal airway mucus impaction.[75–77] MR angiography images with or without the use of gadolinium have been shown to be effective in the depiction of the aberrant arterial supply.[3,75,78]

Management is predominantly surgical given the risk for recurrent infection and the small risk for associated

 © 2014 Lippincott Williams & Wilkins

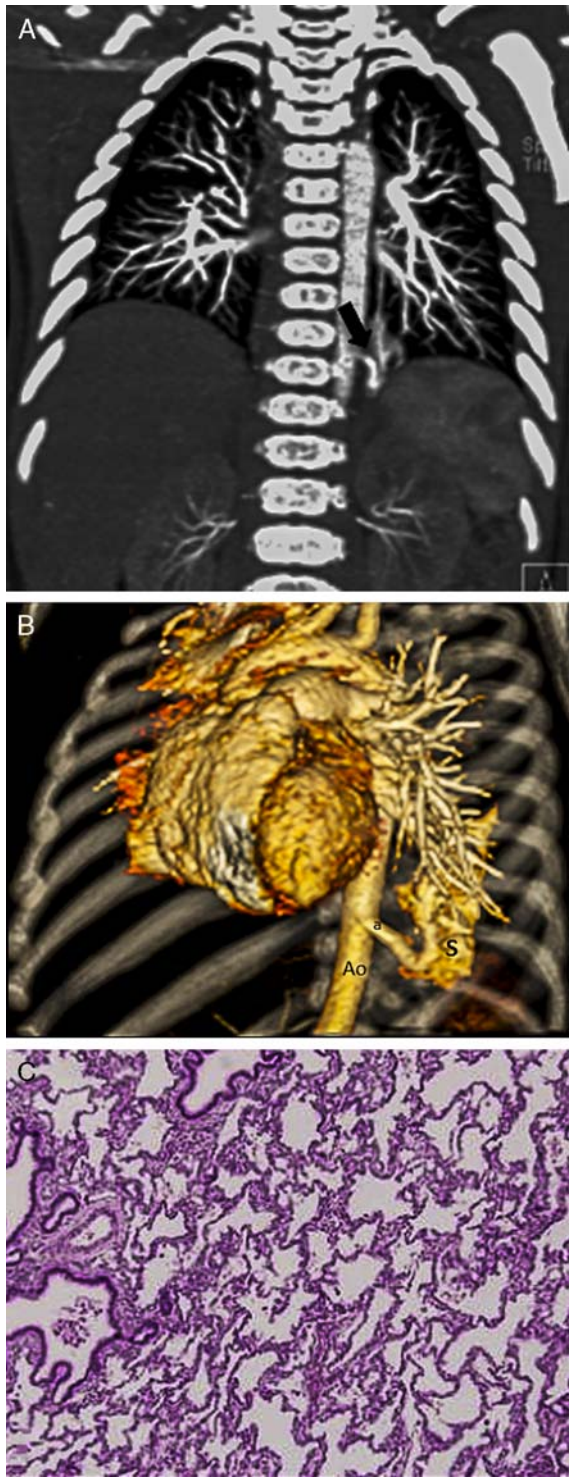

FIGURE 15. A, Coronal reformatted maximum intensity projection image from a contrast-enhanced thoracic CT angiogram reveals a sequestration (arrow) in the medial left lower hemithorax with its feeding vessel (arrow) arising from the aorta. B, Sagittal view from a volume-rendered 3D image demonstrates more clearly the feeding artery (a) arising from the aorta (Ao) and supplying the left lower lobe sequestration (S). C, Medium-power magnification pictomicrograph showing uniformly dilated and simplified alveoli from an extralobar sequestration. full color online

malignancy.[2,30] Recently, embolization of the anomalous arterial supply has been suggested as an alternative to surgery with a reported high rate of success.[3,79,80]

FUTURE DIRECTIONS

Although much knowledge has been gained over the last several decades regarding CLAs, there are still areas that need further elucidation. Precise etiologies remain elusive for a large portion of these lesions. Further research, particularly in molecular biology and genetics, may help shed light into why and when these abnormalities occur. Continued research and utilization of advanced imaging techniques with particular emphasis on nonradiation alternatives may be helpful in future imaging. One particularly fruitful area is in the advancement of chest MR imaging in which imaging times are progressively decreasing with ever-increasing spatial resolution.[12] However, MR remains deficient in lung parenchymal detail when compared with CT, although this particular drawback is currently the subject of research, with recent studies supporting fast-imaging MR sequences as comparable to CT for thoracic abnormalities. Lastly, the establishment of a consensus between our obstetric, pediatric, and surgical colleagues in terms of optimal management for each lesion could be helpful in standardizing practice and ultimately improving patient outcomes.

REFERENCES

1. Costa Junior Ada S, Perfeito JA, Forte V. Surgical treatment of 60 patients with pulmonary malformations: what have we learned? *J Bras Pneumol*. 2008;34:661–666.
2. Lee EY, Dorkin H, Vargas SO. Congenital pulmonary malformations in pediatric patients: review and update on etiology, classification, and imaging findings. *Radiol Clin North Am*. 2011;49:921–948.
3. Thacker PG, Rao AG, Hill JG, et al. Congenital lung anomalies in children and adults: current concepts and imaging findings. *Radiol Clin North Am*. 2014;52:155–181.
4. Biyyam DR, Chapman T, Ferguson MR, et al. Congenital lung abnormalities: embryologic features, prenatal diagnosis, and postnatal radiologic-pathologic correlation. *Radiographics*. 2010;30:1721–1738.
5. Coley BD. Pediatric chest ultrasound. *Radiol Clin North Am*. 2005;43:405–418.
6. Lee EY, Boiselle PM, Cleveland RH. Multidetector CT evaluation of congenital lung anomalies. *Radiology*. 2008;247:632–648.
7. Yanagawa M, Gyobu T, Leung AN, et al. Ultra-low-dose CT of the lung: effect of iterative reconstruction techniques on image quality. *Acad Radiol*. 2014;21:695–703.
8. Singh S, Kalra MK, Shenoy-Bhangle AS, et al. Radiation dose reduction with hybrid iterative reconstruction for pediatric CT. *Radiology*. 2012;263:537–546.
9. Mieville FA, Berteloot L, Grandjean A, et al. Model-based iterative reconstruction in pediatric chest CT: assessment of image quality in a prospective study of children with cystic fibrosis. *Pediatr Radiol*. 2013;43:558–567.
10. Lee EY, Tracy DA, Mahmood SA, et al. Preoperative MDCT evaluation of congenital lung anomalies in children: comparison of axial, multiplanar, and 3D images. *Am J Roentgenol*. 2011;196:1040–1046.
11. Williams G, Coakley FV, Qayyum A, et al. Fetal relative lung volume: quantification by using prenatal MR imaging lung volumetry. *Radiology*. 2004;233:457–462.
12. Gorkem SB, Coskun A, Yikilmaz A, et al. Evaluation of pediatric thoracic disorders: comparison of unenhanced fast-imaging-sequence 1.5-T MRI and contrast-enhanced MDCT. *Am J Roentgenol*. 2013;200:1352–1357.

© 2014 Lippincott Williams & Wilkins

13. Yikilmaz A, Koc A, Coskun A, et al. Evaluation of pneumonia in children: comparison of MRI with fast imaging sequences at 1.5T with chest radiographs. *Acta Radiol*. 2011;52:914–919.
14. Hubbard AM, Adzick NS, Crombleholme TM, et al. Congenital chest lesions: diagnosis and characterization with prenatal MR imaging. *Radiology*. 1999;212:43–48.
15. Beerbaum P, Korperich H, Barth P, et al. Noninvasive quantification of left-to-right shunt in pediatric patients: phase-contrast cine magnetic resonance imaging compared with invasive oximetry. *Circulation*. 2001;103:2476–2482.
16. Fain SB, Korosec FR, Holmes JH, et al. Functional lung imaging using hyperpolarized gas MRI. *J Magn Reson Imaging*. 2007;25:910–923.
17. Altes TA, Salerno M. Hyperpolarized gas MR imaging of the lung. *J Thorac Imaging*. 2004;19:250–258.
18. Lee EY. Advancing CT and MR imaging of the lungs and airways in children: imaging into practice. *Pediatr Radiol*. 2008;38(suppl 2):S208–S212.
19. Riedlinger WF, Vargas SO, Jennings RW, et al. Bronchial atresia is common to extralobar sequestration, intralobar sequestration, congenital cystic adenomatoid malformation, and lobar emphysema. *Pediatr Dev Pathol*. 2006;9:361–373.
20. Langston C. New concepts in the pathology of congenital lung malformations. *Semin Pediatr Surg*. 2003;12:17–37.
21. Talner LB, Gmelich JT, Liebow AA, et al. The syndrome of bronchial mucocele and regional hyperinflation of the lung. *Am J Roentgenol Radium Ther Nucl Med*. 1970;110:675–686.
22. Bagheri R, Asnaashari AM, Afghani R. Esophageal duplication cyst. *Asian Cardiovasc Thorac Ann*. 2014, Apr 22. [Epub ahead of print].
23. Macpherson RI. Gastrointestinal tract duplications: clinical, pathologic, etiologic, and radiologic considerations. *Radiographics*. 1993;13:1063–1080.
24. Zylak CJ, Eyler WR, Spizarny DL, et al. Developmental lung anomalies in the adult: radiologic-pathologic correlation. *Radiographics*. 2002;22:S25–S43.
25. Aktogu S, Yuncu G, Halilcolar H, et al. Bronchogenic cysts: clinicopathological presentation and treatment. *Eur Respir J*. 1996;9:2017–2021.
26. McAdams HP, Kirejczyk WM, Rosado-de-Christenson ML, et al. Bronchogenic cyst: imaging features with clinical and histopathologic correlation. *Radiology*. 2000;217:441–446.
27. Suen HC, Mathisen DJ, Grillo HC, et al. Surgical management and radiological characteristics of bronchogenic cysts. *Ann Thorac Surg*. 1993;55:476–481.
28. Liu YP, Chen CP, Shih SL, et al. Fetal cystic lung lesions: evaluation with magnetic resonance imaging. *Pediatr Pulmonol*. 2010;45:592–600.
29. Ghaye B, Szapiro D, Fanchamps JM, et al. Congenital bronchial abnormalities revisited. *Radiographics*. 2001;21:105–119.
30. Coley BD. *Caffey's Pediatric Diagnostic Imaging*. 12th ed. Philadelphia, PA: Saunders; 2013. 2 v. (xxix, 1616, 1652 p).
31. Ritsema GH. Ectopic right bronchus: indication for bronchography. *Am J Roentgenol*. 1983;140:671–674.
32. Berrocal T, Madrid C, Novo S, et al. Congenital anomalies of the tracheobronchial tree, lung, and mediastinum: embryology, radiology, and pathology. *Radiographics*. 2004;24:e17.
33. Barat M, Konrad HR. Tracheal bronchus. *Am J Otolaryngol*. 1987;8:118–122.
34. Leo F, Galetta D, Borri A, et al. Segmentectomy for carcinoid arising from an accessory cardiac bronchus. *Eur J Cardiothorac Surg*. 2009;35:537.
35. Cho JH, Lee SH, Kim KT, et al. Surgical resection of adenocarcinoma arising from an accessory cardiac bronchus. *Ann Thorac Surg*. 2012;94:1006–1008.
36. Hugosson C, Rabeeah A, Al-Rawaf A, et al. Congenital bilobar emphysema. *Pediatr Radiol*. 1995;25:649–651.
37. Williams HJ, Johnson KJ. Imaging of congenital cystic lung lesions. *Paediatr Respir Rev*. 2002;3:120–127.
38. Karnak I, Senocak ME, Ciftci AO, Buyukpamukcu N.. Congenital lobar emphysema: diagnostic and therapeutic considerations. *J Pediatr Surg*. 1999;34:1347–1351.
39. Ozcelik U, Gocmen A, Kiper N, et al. Congenital lobar emphysema: evaluation and long-term follow-up of thirty cases at a single center. *Pediatr Pulmonol*. 2003;35:384–391.
40. Mei-Zahav M, Konen O, Manson D, et al. Is congenital lobar emphysema a surgical disease? *J Pediatr Surg*. 2006;41: 1058–1061.
41. Azizkhan RG, Crombleholme TM. Congenital cystic lung disease: contemporary antenatal and postnatal management. *Pediatr Surg Int*. 2008;24:643–657.
42. Daltro P, Werner H, Gasparetto TD, et al. Congenital chest malformations: a multimodality approach with emphasis on fetal MR imaging. *Radiographics*. 2010;30:385–395.
43. Cannie M, Jani J, De Keyzer F, et al. Magnetic resonance imaging of the fetal lung: a pictorial essay. *Eur Radiol*. 2008; 18:1364–1374.
44. Hubbard AM, Crombleholme TM. Anomalies and malformations affecting the fetal/neonatal chest. *Semin Roentgenol*. 1998;33:117–125.
45. Wilson RD, Hedrick HL, Liechty KW, et al. Cystic adenomatoid malformation of the lung: review of genetics, prenatal diagnosis, and in utero treatment. *Am J Med Genet A*. 2006;140:151–155.
46. Stocker JT, Madewell JE, Drake RM. Congenital cystic adenomatoid malformation of the lung. Classification and morphologic spectrum. *Hum Pathol*. 1977;8:155–171.
47. Stocker J. Congenital pulmonary airway malformation: a new name for and an expanded classification of congenital cystic adenomatoid malformation of the lung. *Histopathology*. 2002;41:424–431.
48. Newman B. Congenital bronchopulmonary foregut malformations: concepts and controversies. *Pediatr Radiol*. 2006;36: 773–791.
49. Currarino G, Williams B. Causes of congenital unilateral pulmonary hypoplasia: a study of 33 cases. *Pediatr Radiol*. 1985;15:15–24.
50. Ellis K. Fleischner lecture. Developmental abnormalities in the systemic blood supply to the lungs. *Am J Roentgenol*. 1991;156:669–679.
51. Lynch DA, Higgins CB. MR imaging of unilateral pulmonary artery anomalies. *J Comput Assist Tomogr*. 1990;14:187–191.
52. Maldonado JA, Henry T, Gutierrez FR. Congenital thoracic vascular anomalies. *Radiol Clin North Am*. 2010;48:85–115.
53. Fiore AC, Brown JW, Weber TR, et al. Surgical treatment of pulmonary artery sling and tracheal stenosis. *Ann Thorac Surg*. 2005;79:38–46.
54. Ho AS, Koltai PJ. Pediatric tracheal stenosis. *Otolaryngol Clin North Am*. 2008;41:999–1021.
55. Mayhew CE, Lee EE, Balasubramanian S, et al. Chest radiographic findings in pediatric patients with intraluminal pulmonary vein stenosis. *Congenit Heart Dis*. 2014;9:151–157.
56. Lee EY, Jenkins KJ, Muneeb M, et al. Proximal pulmonary vein stenosis detection in pediatric patients: value of multiplanar and 3-D VR imaging evaluation. *Pediatr Radiol*. 2013; 43:929–936.
57. Vyas HV, Greenberg SB, Krishnamurthy R. MR imaging and CT evaluation of congenital pulmonary vein abnormalities in neonates and infants. *Radiographics*. 2012;32:87–98.
58. Ho ML, Bhalla S, Bierhals A, et al. MDCT of partial anomalous pulmonary venous return (PAPVR) in adults. *J Thorac Imaging*. 2009;24:89–95.
59. Srivastava D, Preminger T, Lock JE, et al. Hepatic venous blood and the development of pulmonary arteriovenous malformations in congenital heart disease. *Circulation*. 1995;92:1217–1222.
60. Shah MJ, Rychik J, Fogel MA, et al. Pulmonary AV malformations after superior cavopulmonary connection: resolution after inclusion of hepatic veins in the pulmonary circulation. *Ann Thorac Surg*. 1997;63:960–963.
61. Schraufnagel DE, Kay JM. Structural and pathologic changes in the lung vasculature in chronic liver disease. *Clin Chest Med*. 1996;17:1–15.
62. Lee KN, Lee HJ, Shin WW, et al. Hypoxemia and liver cirrhosis (hepatopulmonary syndrome) in eight patients:

 © 2014 Lippincott Williams & Wilkins

comparison of the central and peripheral pulmonary vasculature. *Radiology*. 1999;211:549–553.
63. McAdams HP, Erasmus J, Crockett R, et al. The hepatopulmonary syndrome: radiologic findings in 10 patients. *Am J Roentgenol*. 1996;166:1379–1385.
64. Lee EY, Siegel MJ, Hildebolt CF, et al. MDCT evaluation of thoracic aortic anomalies in pediatric patients and young adults: comparison of axial, multiplanar, and 3D images. *Am J Roentgenol*. 2004;182:777–784.
65. Wang CC, Wu ET, Chen SJ, et al. Scimitar syndrome: incidence, treatment, and prognosis. *Eur J Pediatr*. 2008;167:155–160.
66. Michailidis GD, Simpson JM, Tulloh RM, et al. Retrospective prenatal diagnosis of scimitar syndrome aided by three-dimensional power Doppler imaging. *Ultrasound Obstet Gynecol*. 2001;17:449–452.
67. Bhide A, Murphy D, Thilaganathan B, et al. Prenatal findings and differential diagnosis of scimitar syndrome and pulmonary sequestration. *Ultrasound Obstet Gynecol*. 2010;35:398–404.
68. Woodring JH, Howard TA, Kanga JF. Congenital pulmonary venolobar syndrome revisited. *Radiographics*. 1994;14:349–369.
69. Konen E, Raviv-Zilka L, Cohen RA, et al. Congenital pulmonary venolobar syndrome: spectrum of helical CT findings with emphasis on computerized reformatting. *Radiographics*. 2003;23:1175–1184.
70. Yikilmaz A, Lee EY. CT imaging of mass-like nonvascular pulmonary lesions in children. *Pediatr Radiol*. 2007;37:1253–1263.
71. Epelman M, Kreiger PA, Servaes S, et al. Current imaging of prenatally diagnosed congenital lung lesions. *Semin Ultrasound CT MR*. 2010;31:141–157.
72. Panicek DM, Heitzman ER, Randall PA, et al. The continuum of pulmonary developmental anomalies. *Radiographics*. 1987;7:747–772.
73. van Belle A, Buller HR, Huisman MV, et al. Effectiveness of managing suspected pulmonary embolism using an algorithm combining clinical probability, D-dimer testing, and computed tomography. *JAMA*. 2006;295:172–179.
74. Kang M, Khandelwal N, Ojili V, et al. Multidetector CT angiography in pulmonary sequestration. *J Comput Assist Tomogr*. 2006;30:926–932.
75. Au VW, Chan JK, Chan FL. Pulmonary sequestration diagnosed by contrast enhanced three-dimensional MR angiography. *Br J Radiol*. 1999;72:709–711.
76. Hang JD, Guo QY, Chen CX, et al. Imaging approach to the diagnosis of pulmonary sequestration. *Acta Radiol*. 1996;37:883–888.
77. Naidich DP, Rumancik WM, Ettenger NA, et al. Congenital anomalies of the lungs in adults: MR diagnosis. *Am J Roentgenol*. 1988;151:13–19.
78. Lehnhardt S, Winterer JT, Uhrmeister P, et al. Pulmonary sequestration: demonstration of blood supply with 2D and 3D MR angiography. *Eur J Radiol*. 2002;44:28–32.
79. Lee KH, Sung KB, Yoon HK, et al. Transcatheter arterial embolization of pulmonary sequestration in neonates: long-term follow-up results. *J Vasc Interv Radiol*. 2003;14:363–367.
80. Lee BS, Kim JT, Kim EA, et al. Neonatal pulmonary sequestration: clinical experience with transumbilical arterial embolization. *Pediatr Pulmonol*. 2008;43:404–413.

Questions marked with an asterisk are ABR Self-Assessment Module (SAM) questions. Participants can claim credit for the SAM regardless of the test outcome. Notify the ABR of the SAM completion, or visit the ABR website at www.theabr.org to set up or login to your personal database to record the number of SAMs you completed. The SAM ID number will be printed on the CME certificate for your records. If you wish to include the ID number in your ABR database, contact a MOC Specialist at the ABR office for instruction by calling 520-519-2152.

© 2014 Lippincott Williams & Wilkins